

Self-tracking in solvent-free, low-dimensional polymer electrolyte blends with lithium salts giving high ambient DC conductivity†

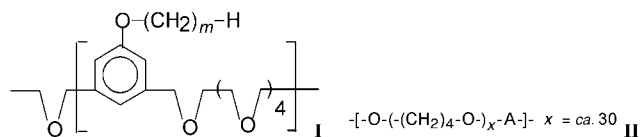
Yungui Zheng, Fusong Chia, Goran Ungar and Peter V. Wright*

Department of Engineering Materials, University of Sheffield, Sheffield, UK S1 3JD.
E-mail: p.v.wright@sheffield.ac.uk

Received (in Cambridge, UK) 24th May 2000, Accepted 26th June 2000
Published on the Web 13th July 2000

A solvent-free, low-dimensional polymer electrolyte blend is described demonstrating a novel process of 'self-tracking' along the field direction in DC polarisation between lithium electrodes and giving ambient DC and AC conductivities upto 10^{-3} S cm^{-1} with low temperature dependence of conduction.

Solvent-free polymer electrolytes have been based largely upon complexes of lithium salts in amorphous forms of poly(ethylene oxide) (PEO).^{1–3} However, their application in ambient temperature batteries, requiring conductivities of *ca.* 10^{-3} S cm^{-1} , has been prohibited due to their low ambient temperature conductivities. Other amorphous systems giving conductivities between 10^{-4} – 10^{-5} S cm^{-1} have been proposed.^{4,5} With a view to creating low impedance pathways and inhibiting ion aggregates we have adapted the extended helical crystalline structures of PEO–alkali salt complexes^{6–8} to synthesise organised low-dimensional polymer complexes^{9–13} with amphiphilic polymers poly[2,5,8,11,14-pentaoxapentadecamethylene(5-alkoxy-1,3-phenylene)] coded *CmO5* (I).



When $m = 16$, (C16O5), sidechains interdigitate in a hexagonal lattice layer between polyether helices in which cations are encapsulated, one per repeat unit/helical turn, in equimolar complexes denoted, *e.g.* C16O5:LiClO₄ (1:1). Anions lie in the interhelical spaces. (*cf.* Fig. 1) and interlamellar long spacings of 40–45 Å are observed.^{9,10,11}

Here, we report enhanced ambient conduction in solvent-free LiClO₄ and LiClO₄/LiBF₄ complexes of *CmO5* blended with a second copolymer of poly(tetramethylene oxide) (II). The *n*-alkyl side chains R in I are either C₁₆H₃₃ (C16O5) or a random

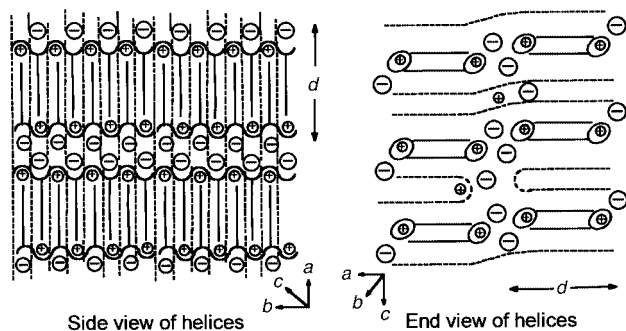


Fig. 1 Schematic molecular structure of C16O5:II:LiClO₄. Solid lines: C16O5, dashed lines: polymer II.

† Electronic supplementary information (ESI) available: a molecular dynamics model with coloured atoms of the C16O5:II:Li salt complex from Cerius² software. See <http://www.rsc.org/suppdata/cc/b0/b004174m/>

equimolar copolymer mixture with C₁₂H₂₅ (C16C12O5). In II the units -A- are either -CH₂- (denoted IID1) or -CH₂C(=CH₂)CH₂- (denoted IID4). Both I and II are prepared to high molar mass ($\langle M_w \rangle = 8 \times 10^4$ and 4×10^4 respectively) giving thin films with good mechanical properties.

Polymers I^{9,10} and II were prepared by standard Williamson condensations and complexes were prepared by mixing polymer I (1 mol repeating unit), polymer II (7 mols of -(CH₂)₄-O-) units) and either LiClO₄ (1.5 mol) or LiClO₄ / LiBF₄ (0.75/0.75) from mixed dichloromethane/acetone solvent. The heptamer segment for the stoichiometric equivalent of polymer II for each repeat unit of I is indicated by a molecular dynamics model.† The molar compositions of complexed blends are therefore denoted I:II:Li salt (1:1:1.5) where the second digit denotes the mol of heptamer segment. The schematic model (Fig. 1) and the molecular model† are consistent with small-to-wide angle X-ray analysis and with DSC which indicate that the strands of polymer II disrupt the alkyl sidechains of polymer I. Sidechain melting temperatures are reduced by *ca.* 10 °C by blending with II. C16O5:II:LiClO₄ melts at *ca.* 34 °C at the peak. Complexes with mixed $m = 16/12$ sidechains (C16C12O5) melt at *ca.* 24 °C. The pure polymers II melt at 20 °C.

Fig. 2 shows isothermal DC‡ conductivity *vs.* time in cells with Li electrodes (Li|I/II–LiClO₄|Li) for C16O5:II:LiClO₄ (1:1:1.5) polarised with 10 mV at 30 °C, Fig. 2(a), and C16O5:II:LiClO₄:LiBF₄ (1:1:0.75:0.75) polarised with 100 mV at 25 °C, Fig. 2(b). In a novel 'self-tracking process' the current increases stepwise over *ca.* 24 h corresponding to Li⁺ conductivity increasing from *ca.* 10^{-6} S cm^{-1} to *ca.* 10^{-3} S cm^{-1} .

The DC data are supported by AC complex impedance measurements for C16O5:II:LiClO₄ (1:1:1.5) and C16C12O5:II:LiClO₄ (1:1:1.5) between ITO electrodes as shown in Fig. 3(a) and (b) as $\log \sigma$ *vs.* $1/T$. From lower levels at ambient temperatures all three systems undergo similar 'transitions' on heating to *ca.* 100 °C after which ambient conductivities between $2\text{--}6 \times 10^{-4}$ S cm^{-1} are observed. In

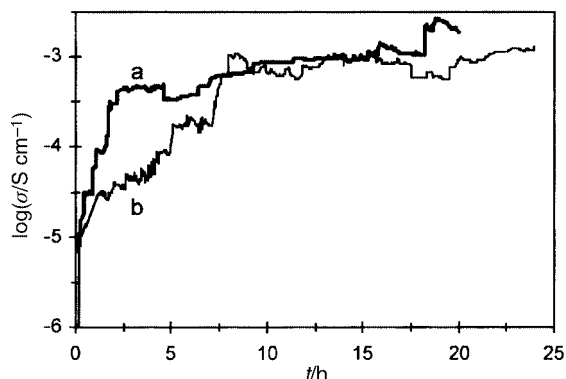


Fig. 2 DC polarisation between lithium electrodes. (a) C16O5:IID4:LiClO₄ (1:1:1.5), 10 mV at 30 °C, 450 μm . (b) C16O5:IIIC1:LiClO₄:LiBF₄ (1:1:0.75:0.75), 100 mV at 25 °C, 100 μm .

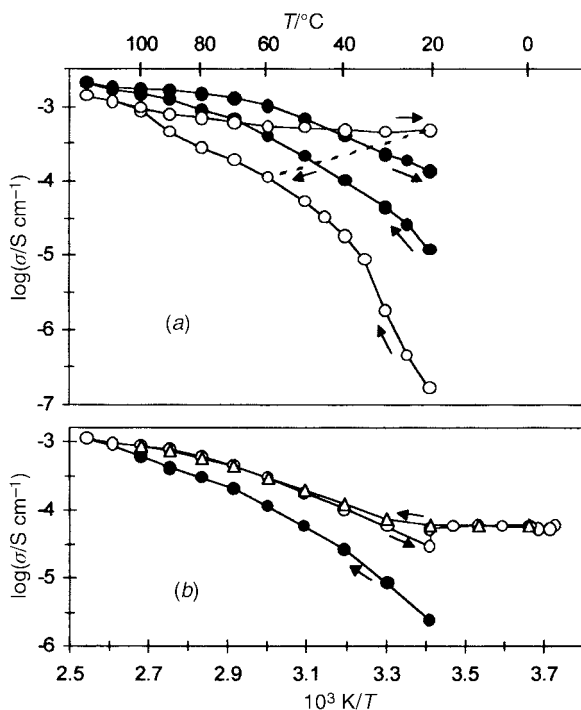


Fig. 3 Temperature dependence of AC conductivities between ITO electrodes. Arrows indicate the direction of heating. (a) C16O5:IIIC1:LiClO₄ (1:1:1.5) (—○—) and C16C12O5:IIIC1:LiClO₄ (1:1:2) (—●—) Cell thicknesses are 100 μm. (b) C16O5:IID4:LiClO₄ (1:1:1.5) Heating (—●—), cooling (—○—) and reheating (—△—). Cell thickness is 50 μm.

Fig. 3(b) the ambient conductivity is slightly lower at 8×10^{-5} S cm⁻¹ after an isothermal increase over ca. 12 h at 20 °C but this level of conductivity is remarkably maintained down to -5 °C. The cooling runs of the C16O5 systems also demonstrate virtual temperature independence (temperature-independent conductivities at the level of 10^{-7} – 10^{-6} S cm⁻¹ have previously been observed¹³ in Langmuir–Blodgett films of a variety of C16O5–Li salt complexes). However, whereas the ‘cooling data’ are unstable on re-heating above the sidechain melting temperature (ca. 35 °C), returning to the lower initial heating curve, Fig. 3(a), the data in Fig. 3(b) demonstrate that on cooling below the side chain melting endotherm (lower limit 20 °C) stable and reversible conductivities may be observed.

The possibility that Li dendrite formation has a significant influence on these and a number of other DC polarisations reproducing these results is not supported by comparisons with observed¹⁴ dendritic growth in conventional amorphous polymer electrolyte systems. In contrast to the latter the tracking phenomenon commences almost from the outset with very low current densities (ca. 0.1 μA cm⁻²) and without cycling. Furthermore, the maximum conductivities (ca. 10^{-3} S cm⁻¹)

are reproduced over a wide range of final current densities. In Fig. 2(b) (100 mV and 100 μm cell thickness) the current density is 45 times greater than in Fig. 2(a) (10 mV and 450 μm thickness, 0.2 mA cm⁻² maximum).

It is anticipated that polymer II (with the more extensive skeletal domain) will promote orientation of conducting planes *bc* in the direction normal to the electrodes when the blend is subjected to mechanical shear in the plane of the film (parallel to the electrodes). The ion current may perhaps assist such orientations by a ‘melting–recrystallisation’ reorganisation within the sidechain melting endotherm (20–35 °C). However, imposition of the field is expected to bring about a new steady state redistribution of ions between the channels of polymer I and the polymer II environment promoting vacancies in I in which ions are presumed the more mobile ($\sigma = 7 \times 10^{-7}$ S cm⁻¹ for complexes of pure II with LiClO₄ at 25 °C). The relative mobilities and stabilities of ions in I and II and the identification of premelting (order–disorder) transitions which could account for the low temperature dependence of conductivity are subjects of further work.

We acknowledge financial support for this work from the Engineering and Physical Science Research Council.

Notes and references

‡ For DC measurements Li electrodes were prepared under argon from freshly-pressed Li pellets (ca. 2 mm diam.) in paraffin oil and cells were assembled under argon with polyethylene separators. DC and AC measurements using cellulose acetate separators were performed under vacuum using a Solartron 1287 Electrochemical Interface with a Solartron 1250 Frequency Response Analyser 1–64 kHz.

- 1 *Polymer Electrolyte Reviews 1*, ed. J. R. MacCallum and C. A. Vincent, Elsevier Applied Science, London, 1987.
- 2 *Polymer Electrolyte Reviews 2*, ed. J. R. MacCallum and C. A. Vincent, Elsevier Applied Science, London, 1989.
- 3 F. M. Gray, *Polymer Electrolytes*, Materials Monographs, The Royal Society of Chemistry, Cambridge, 1997.
- 4 C. A. Angell, C. Liu and E. Sanchez, *Nature*, 1993, **362**, 137.
- 5 F. Croce, C. Appetecchi, L. Persi and B. Scrosati, *Nature*, 1998, **394**, 456.
- 6 Y. Chatani and S. Okamura, *Polymer*, 1987, **28**, 1815.
- 7 P. Lightfoot, M. A. Mehta and P. G. Bruce, *Science*, 1993, **262**, 883.
- 8 Y. G. Andreev, P. Lightfoot and P. G. Bruce, *J. Appl. Crystallogr.*, 1997, **18**, 294.
- 9 F. B. Dias, J. P. Voss, S. V. Batty, P. V. Wright and G. Ungar, *Macromol. Rapid Commun.*, 1994, **15**, 961.
- 10 F. B. Dias, S. V. Batty, G. Ungar, J. P. Voss and P. V. Wright, *J. Chem. Soc., Faraday Trans.*, 1996, **92**, 2599.
- 11 P. V. Wright, Y. Zheng, D. Bhatt, T. Richardson and G. Ungar, *Polym. Int.*, 1998, **47**, 34.
- 12 Y. Zheng, P. V. Wright and G. Ungar, *Electrochim. Acta*, 2000, **45**, 1161.
- 13 Y. Zheng, A. Gibaud, N. Cowlam, T. H. Richardson, G. Ungar and P. V. Wright, *J. Mater. Chem.*, 2000, **10**, 69.
- 14 C. Brissot, M. Rosso, J.-N. Chazalviel and S. Lascaud, *J. Power Sources*, 1999, **81–82**, 925.